

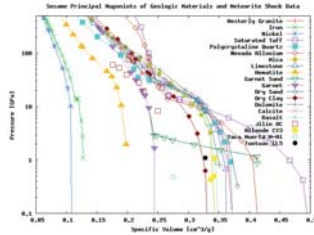
# Material Models of Small Solar System Bodies for use in Impact Hazard Mitigation Modeling.

C. S. Plesko, J. M. Ferguson, G. R. Gisler, and R. P. Weaver

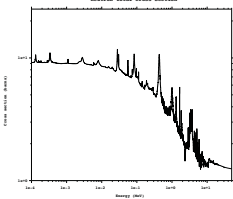
Computer models of the deflection and disruption of potentially hazardous objects (PHOs) require detailed material models in order to accurately predict the response of the target. A wealth of data on the composition of asteroids and comets has been returned directly from missions in situ (e.g. S. A. Stern 2011), and Earth-based experiments (e.g. Furnish et al. 2013). Here we compare available data from meteorites and small solar system bodies to analogue EOS's available in the public Los Alamos National Laboratory SESAME EOS database to explore the applicability and limitations of these models. We also use the composition data from meteorite and sample return analysis (e.g. Ebihara et al. 2011) to explore the potential response of PHO material types to neutron bombardment in MCNP and the ENDF neutron cross-section libraries, and attempt to provide recommendations on how to best approximate our current understanding of small solar system body composition in particle transport codes.

**Motivation:** We are interested in modeling small solar system bodies in impacts and impact hazard mitigation scenarios. (See presentations by Gisler and Weaver, PDC 2015.) We use a two-phased approach. For nuclear deflection we first use a particle transport code to model neutron energy deposition. To do so accurately, we need to know the chemical composition of the target, and how that might vary over spectral type. We then assume the predicted amount of internal energy as a function of location as the starting condition for a hydrocode model. Hydrocodes move mass, momentum, and energy on a mesh. This system of equations is closed by an equation that describes the pressure, temperature, and specific volume state (EOS) of a given material.

**The Sesame EOS Database:** EOSs relate the pressure (P), temperature (T), and specific volume ( $V = 1/\rho$ ) of a material, using the Rankine-Hugoniot jump conditions, which predict P, V, and T across a shock. The principal Hugoniot is a collection of single-shock states starting from  $P, T = 0$ . The Sesame database contains 20 geologic materials, each of which is composed of tables with 100's to 1000's of table points describing the material's behavior. The relevant materials for meteoritic models are shown to the right.

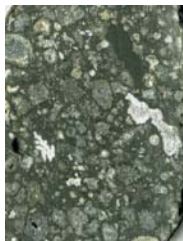


**MCNP:** Monte Carlo N-Particle transport code is a general-purpose particle transport code commonly used to model neutron, photon, and electron transport for medical physics, reactor design, accelerator target and detector design, and a variety of other applications. It was used to model the propagation of epithermal neutrons through the Martian regolith (Prettyman 2002). It uses current nuclear cross section data where available, and fills in the gaps with analytical models where data are not available. Computational methods are required to calculate neutron energy deposition because the mean free path of a neutron in a solid may be very complicated, as shown by the CI Chondrite cross-section on the left.

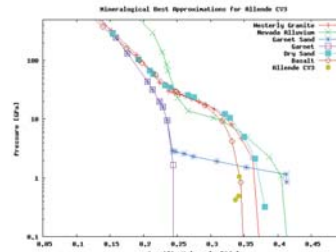


**Available Meteorite Data:**

- Detailed isotopic analysis for transport code cross-sections are available for some samples (e.g. Ebihara et al. 2011).
- Shock Hugoniot data for hydrocode EOS's must be experimentally determined, and those methods are destructive at moderate to high pressures.
- Meteorite shock data is currently sparse.
- Dai et al. (1997) conducted 10 gas gun impact experiments on samples from the Jilin ordinary chondrite.
- Furnish et al. (2013) used the Sandia Z-machine to obtain data on
  - Allende (CV3 Chondrite)
  - One point each:
    - Vaca Muerta (Mesosiderite-A1)
    - Tuxtlauc (LL5 chondrite)



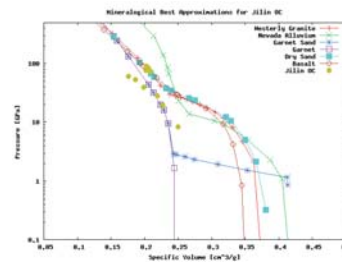
Allende meteorite, photograph by J. St. John, Wikimedia Commons.



**Allende CV3 EOS Match:**  
The Allende meteorite is composed of 25% nickel iron, with olivine, pyroxene, and chondrules making up the rest. It appears to best match the EOSs for Sesame basalt. Allende's metallic component may be drawing the shock data towards the origin in P-V space relative to the non-metallic basalt Hugoniot because it increases the initial density (decreases  $V, V=1/\rho$ ) and decreases the PdV work required to compress the sample to a given final density.

**Jilin Ordinary Chondrite EOS Match:**

The Jilin meteorite is composed of bronselite (a pyroxene), olivine, orthopyroxenes, plagioclase, metals, and sulfides. It appears to best match the EOSs for Sesame garnet, and garnet sand, which may be an effect of garnet's status as an orthosilicate, like olivine. Dai et al.'s data also contained some points matching other silicates that contain little or no water. These may be off-Hugoniot data that experienced multiple shocks before the measurement was taken, or they could have somewhat different compositions from the other samples, assuming small-scale heterogeneity.

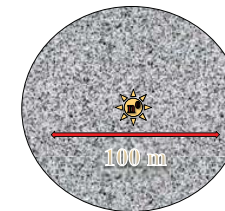


Further experimental work is required, even on the relatively comprehensive Jilin dataset. The size of the samples used for these experiments are on the mm- to cm- scale, which is the same scale as the compositional heterogeneity of the meteorites. This may affect the results of individual experiments in ways that may not be readily distinguished from problems with individual experiments such as pre-measurement shock ring-up.

**Conclusions:**

- Meteoritic shock data is sparse
- Sample composition is variable
- Equations of state will always be uncertain over a meter- or kilometer-sized PHO
- Mineral weighted EOSs are a useful approximation
- Meteoritic metal content
  - increases sample starting density,
  - decreases shock pressure relative to metal-poor analogs because it takes less work to compress the material to a given density
- EOS's of metal-poor terrestrial rocks of otherwise similar composition may under-estimate the density and over-estimate pressure and temperature of the Hugoniot shock state, over-estimating vapor production and momentum transfer.
- Analytically estimated mixed-material EOSs are possible, but they will miss the dispersion in sample data.

**Particle Transport Models:** These models consist of 100 m-diameter spheres of target material with a point neutron source at the center, so all of the neutrons released by the source are absorbed by the target. This is done for simplicity, not to be a realistic deflection geometry. The neutron sources are either a mono-energetic 14 MeV source, or use the source spectrum from White et al. (2001). Each model was run with 1 billion particle histories.



**Neutron Interaction Results:** The mean free path and number of collisions per source particle are higher for higher energy neutrons. The energy mediated by these neutrons is deposited over a region that is about 1-2 MFP's thick. The CI Chondrite target captures neutrons more readily because it contains more hydrogen than either of the other materials. Higher energy neutrons deposit more energy, but over many more collisions, unless a strong capture resonance like hydrogen is part of the material's cross-section.

	Neutron Mean Free Path (MFP)		Avg. Collisions / Particle	
	White et al.	14 MeV	White et al.	14 MeV
Basalt	9.6 cm	11.8 cm	55	70
CI Chondrite	2.7 cm	10.4 cm	19	28
Itokawa	8.9 cm	11.5 cm	62	96

**Activation Results:** The activation products predicted to be produced in a nuclear deflection attempt come from two sources, one, the device itself, is device dependent. The second is activation products from the target itself. Higher energy 14 MeV neutrons tend to produce more activation products than lower energy neutrons (Glasstone and Dolan, 1977). Activation products of interest for an object like Itokawa grain 49-1 would be produced in small amounts, shown below, most of which would disperse radially from the burst location as a high-velocity vapor.

**Predicted Activation Products for Objects Like Itokawa Grain 49-1**

Isotope	Half life	[g/kt], White et al.	[g/kt] 14 MeV
<sup>55</sup> Fe	2.7 years	8.98e-8	0.008
<sup>60</sup> Co	5.3 years	0.016	0.004
<sup>59</sup> Ni	76,000 years	0.026	0.004
<sup>65</sup> Zn	243 days	8.37e-5	0.019
<sup>151</sup> Sm	90 years	5.18e-10	0.045
<sup>153</sup> Sm	2 days	0.062	0.045
<sup>150</sup> Eu	36.9 years	8.59e-9	0.045
<sup>152</sup> Eu	13 years	1.95	0.045
<sup>192</sup> Ir	73.8 days	5.12e-13	0.057